ACS APPLIED MATERIALS & INTERFACES

Research Article

www.acsami.org

Characterization of Sulfur Bonding in CdS:O Buffer Layers for CdTe-based Thin-Film Solar Cells

Douglas A. Duncan,[*,†,‡] Jason M. Kephart,[§] Kimberly Horsley,[†] Monika Blum,[†,∥] Michelle Mezher,[†] Lothar Weinhardt,[†,⊥,#,▽] Marc Häming,[†,#] Regan G. Wilks,[‡] Timo Hofmann,[†,◆] Wanli Yang,[∥] Marcus Bär,[†,‡,⊗] Walajabad S. Sampath,[§] and Clemens Heske[*,†,⊥,#,▽]

[†]Department of Chemistry and Biochemistry, University of Nevada, Las Vegas (UNLV), Las Vegas, Nevada 89154-4003, United States

[‡]Renewable Energy, Helmholtz-Zentrum Berlin für Materialien und Energie GmbH, 14109 Berlin, Germany

[§]Department of Mechanical Engineering, Colorado State University, Fort Collins, Colorado 80523, United States

[∥]Advanced Light Source, Lawrence Berkeley National Laboratory, Berkeley, California 94720, United States

[⊥]ANKA Synchrotron Radiation Facility, Karlsruhe Institute of Technology (KIT), 76344 Eggenstein-Leopoldshafen, Germany

[#]Institute for Photon Science and Synchrotron Radiation, Karlsruhe Institute of Technology (KIT), 76344 Eggenstein-Leopoldshafen, Germany

[▽]Institute for Chemical Technology and Polymer Chemistry, Karlsruhe Institute of Technology (KIT), 76128 Karlsruhe, Germany

[⊗]Institut für Physik und Chemie, Brandenburgische Technische Universität Cottbus-Senftenberg, 03046 Cottbus, Germany

ABSTRACT: On the basis of a combination of X-ray photoelectron spectroscopy and synchrotron-based X-ray emission spectroscopy, we present a detailed characterization of the chemical structure of CdS:O thin films that can be employed as a substitute for CdS layers in thin-film solar cells. It is possible to analyze the local chemical environment of the probed elements, in particular sulfur, hence allowing insights into the species-specific composition of the films and their surfaces. A detailed quantification of the observed sulfur environments (i.e., sulfide, sulfate, and an intermediate oxide) as a function of oxygen content is presented, allowing a deliberate optimization of CdS:O thin films for their use as alternative buffer layers in thin-film photovoltaic devices.

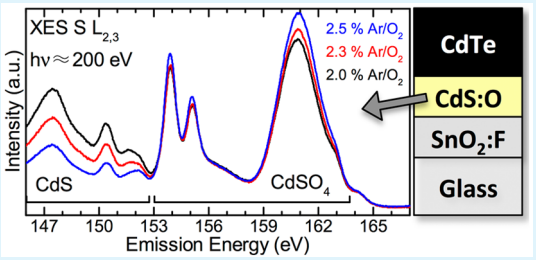

KEYWORDS: *solar cells, CdS, CdTe, alternative buffer layers, XPS*

1. INTRODUCTION

Although Si-based devices currently dominate photovoltaic power production, thin-film devices based on CdTe have achieved a notable market share as a cost-effective alternative (with current world-record cell efficiency of 21.0%).[1] For further improvement, efforts focus on the fact that absorption in the CdS buffer layer of such cells reduces the flux of high-energy photons to the CdTe absorber. This parasitic light absorption can result in more than 10% loss in short-circuit current density.[2] One way to prevent this loss is to increase the band gap of the buffer material, e.g., by incorporating oxygen during RF sputtering of CdS (such as by introducing O_2 into the Ar flow).[3−8] Other methods have been successfully used for chalcopyrite thin-film solar cells;[9−12] however, only very recently has detailed work been performed on CdS:O thin films.[6−8] For CdTe, this process has produced devices with efficiencies above 15%.[3,5,8,13] To optimize the buffer properties and to improve further device performance, a detailed understanding of the electronic and chemical structure is required. Soo et al.[14] have shown the bulk of such films to consist of oxygen-free CdS nanocrystals and S−O complexes, which are speculated to be SO_3^{2-} and SO_4^{2-} complexes. To analyze the chemical structure of the S−O complexes in detail, X-ray photoelectron spectroscopy (XPS) and soft X-ray emission spectroscopy (XES) were used to study the species-specific composition of the surface and bulk, respectively. We thus derive the impact of oxygen incorporation into CdS thin films, monitoring the relative intensities of the various sulfur species at the surface and bulk as a function of O content. The results allow for deeper insights into, and deliberate optimization of, such CdS:O thin films in solar devices.

2. EXPERIMENTAL SECTION

$CdSO_x$/SnO:F/glass layer stacks were grown at CSU using RF sputtering. O_2 gas (99.999%) was introduced into the Ar flow of the sputter gas. On the basis of deposition time, the expected thickness of the $CdSO_x$ films is 100 nm. The amount of O_2 incorporated is related to its flow rate relative to Ar. Here, we chose an oxygen content (2.3%

Received: April 23, 2015
Accepted: July 6, 2015
Published: July 6, 2015

© 2015 American Chemical Society

DOI: 10.1021/acsami.5b03503
ACS Appl. Mater. Interfaces 2015, 7, 16382−16386

O_2 flow rate relative to Ar) that was optimal in terms of stability toward subsequent high-temperature processing and avoided the presence of a kink in the $J-V$ characteristics. Furthermore, two films were produced with slightly different O contents (2.0 and 2.5%). A detailed investigation of the impact of O content on transparency, quantum efficiency, and device performance is given in ref 5.

For the present study, Tec 10-coated 3.2 mm float glass substrates (Pilkington[4,5]) were used. After production, the samples were vacuum-sealed under dry nitrogen, without exposure to air, and shipped to UNLV for characterization. The samples were unpacked in the inert environment of a dry nitrogen-filled glovebox and directly introduced into the ultrahigh vacuum (UHV) system with a base pressure below 5×10^{-10} mbar. X-ray photoelectron spectroscopy (XPS) was performed using a twin-anode Al Kα/Mg Kα X-ray source (Specs XR-50) and a Scienta R4000 electron analyzer; the energy scale was calibrated in accordance with ISO 15472.[15]

X-ray emission spectroscopy (XES) of the S $L_{2,3}$ edge was performed at Beamline 8.0.1.2 of the Advanced Light Source (ALS), Lawrence Berkeley National Laboratory, employing the SALSA endstation with a custom-designed, high-transmission soft X-ray spectrometer.[16,17] To transfer the samples to ALS, they were vacuum-sealed without air exposure, unpacked in the inert environment of a dry nitrogen-filled glovebag and directly introduced into the experimental station (base pressure below 1×10^{-8} mbar). To minimize beam damage effects, the sulfite and sulfate reference powders were scanned in the beam.

3. RESULTS AND DISCUSSION

Mg Kα XPS survey spectra of the as-received CdS:O surfaces (Figure 1) display all expected photoemission and Auger lines

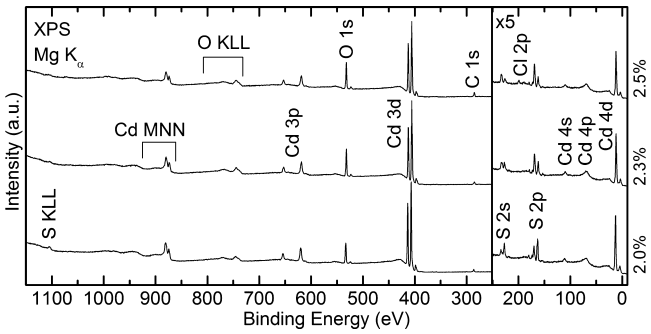

Figure 1. Mg Kα XPS survey spectra of three CdS:O films with O_2/Ar flow rate ratios of 2.0, 2.3, and 2.5% (as labeled on the right ordinate). All photoemission and Auger electron emission lines are labeled, and the spectra are magnified by a factor of 5 for binding energies below 250 eV.

(of Cd, S, and O). We also find a small C 1s contribution, which is likely due to residual carbon contaminants in the 15 mTorr Ar environment of the CdS:O RF sputter deposition chamber. The intensities were magnified by a factor of 5 for binding energies below 250 eV to show a splitting of the S 2s and 2p lines, which will be discussed in more detail in the following. Furthermore, we find that the O 1s signal increases and the Cd signals decrease in intensity with increased oxygen flow rate, as expected, and observe the presence of a Cl contamination on the 2.5% sample.

A detailed measurement of the S 2p region (Figure 2, blue circles) suggests the presence of at least three sulfur species. To analyze the relative binding energy differences between them, the peak center of the lowest-binding energy species (attributed to CdS) was set to zero in all spectra, requiring spectral shifts of 1.5 eV or less. This approach also mitigates any impact of surface band-bending, doping, and (if present) charging effects.

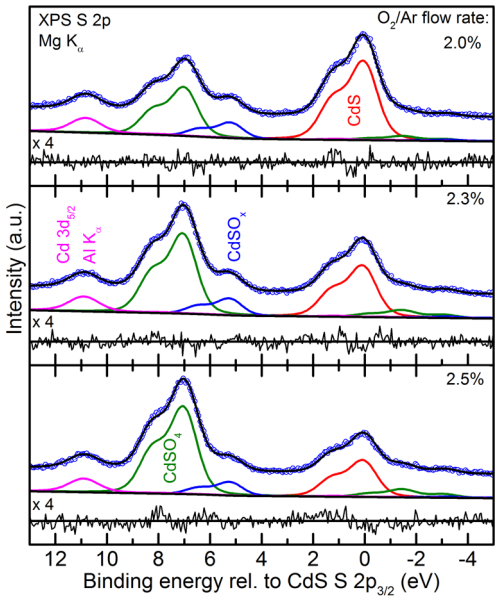

Figure 2. S 2p Mg Kα XPS spectra (blue dots) of three CdS:O films with O_2/Ar flow rate ratios of 2.0, 2.3, and 2.5%. The spectra are referenced to the binding energy of the S $2p_{3/2}$ line of CdS, and described by spectral components representing CdS (red), $CdSO_X$ (blue), $CdSO_4$ (green), Cd $3d_{5/2}$ (excited by Al Kα, magenta). The sum of the fit functions is also shown in blue. Each component consists of two Voigt functions, describing the S 2p spin–orbit doublet and a contribution at lower binding energies that originates from the Mg K$\alpha_{3,4}$ satellites excitations of each line. Below each spectrum, the residuum of each fit is shown, magnified by a factor of 4.

At high binding energies, the spectra are composed of S 2p contributions consistent with a $CdSO_4$ environment[19] (green), ~7 eV shifted with respect to CdS (red), and an intermediate oxide shifted by ~6 eV and labeled "$CdSO_x$" (blue). The chemical shift of this intermediate oxide is consistent with other sulfite species,[18−20] but it requires a detailed analysis of the XES spectra (see below) to derive additional evidence to suggest that this species is indeed a $CdSO_3$ (note that no XPS reference spectra for $CdSO_3$ could be found in an extensive literature search). For the three samples it is seen that, roughly, the CdS contribution decreases and the $CdSO_4$ contribution increases with increased oxygen flow rate, as expected. The intermediate oxide, $CdSO_x$, remains approximately constant despite the increased oxygen incorporation.

To derive a detailed quantification, we note that it is not feasible to simply integrate the area under the spectra, since the lines of the different sulfur species overlap. Instead, a detailed and thorough fit analysis, using a sulfur spin–orbit doublet for each species, is required. Furthermore, all three spectra need to be fitted simultaneously, for which we used the Fityk fitting software.[21] Each species in Figure 2 was described by a sum of eight coupled Voigt functions (red, green, and blue lines) to account for the spin–orbit splitting (with a ratio of 2:1 for the S $2p_{3/2}$ and $2p_{1/2}$ line, respectively) and to include the Mg K$\alpha_{1,2}$ main line as well as the K$\alpha_{3,4}$ satellite excitations. The relative areas and energies were set according to Molder et al.,[18] whereas the Gaussian and Lorentzian widths, respectively, were identical for all species (and used as two free fit parameters). A linear background was simultaneously fitted, and a small Al Kα-excited Cd $3d_{5/2}$ photoemission peak (magenta) was also included to account for X-ray source crosstalk. In total, the three spectra were simultaneously fitted with 20 free parameters

DOI: 10.1021/acsami.5b03503
ACS Appl. Mater. Interfaces 2015, 7, 16382−16386

(out of a total of 480 variables). The resulting fits give an excellent description of the experiment, as is evidenced by the predominantly statistical nature of the residua shown under each spectrum (magnified by a factor of 4) in Figure 2.

The surface composition (Figure 3, left ordinate) was calculated using the area percentage of the different species in

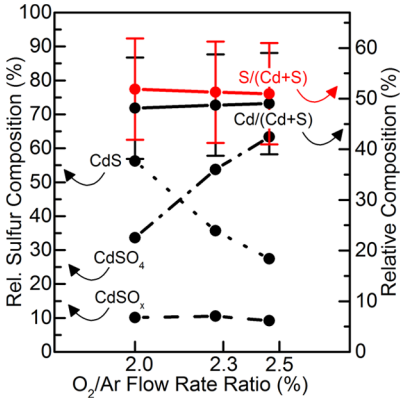

Figure 3. Left ordinate: relative sulfur composition for the CdS (dotted), $CdSO_4$ (dash-dotted), and $CdSO_x$ (dashed) spectral component as a function of O_2/Ar flow rate ratio. Error bars (not shown) are ±2 abs % or less. Right ordinate: relative composition of Cd (Cd/(Cd+S), black) and S (S/(Cd+S), red) for all three samples.

the fit. The CdS and $CdSO_4$ composition at the surface both have a linear dependence on O_2/Ar flow rate across this range, whereas the intermediate, $CdSO_x$, is constant. In this particular series, films leading to the best solar cell performance were made with a 2.3% O_2/Ar flow rate, which, according to Figure 3, represents a slightly $CdSO_4$-rich surface. A detailed analysis of the impact of various preparation parameters on solar cell performance in other sample series is given in ref 5.

To determine the relative composition of S and Cd, we analyzed the intensity of the Al Kα-excited Cd $3d_{5/2}$ line and the total S intensities by using calculated cross sections,[22] taking the relative intensity of the Al Kα-excitation into account (as derived from a separate measurement of a gold reference), and by assuming that the transmission function and attenuation lengths are constant over this narrow energy window. We find that the relative composition of Cd and S (Figure 3, right ordinate) is varying only slightly for the three samples (and well within the error bars of determining the absolute values). This indicates that, at increasing O_2 flow rates, no significant formation of other oxygen-containing cadmium species (e.g., CdO or $Cd(OH)_2$) is found (if present, this would lead to a variation of the Cd/S ratio). Instead, increased O_2 flow rates apparently lead to the formation of oxide species that include both sulfur and cadmium.

To gain more detailed insights into the chemical environment of the sulfur atoms, in particular regarding the intermediate oxide, we recorded S $L_{2,3}$ X-ray emission spectra using high-brilliance synchrotron radiation.

For CdS, the 1/e-attenuation length of the exciting (200 eV) and emitted (ca. 150 eV) photons are approximately 100 and 370 nm, respectively.[23] For $CdSO_4$, the corresponding values vary according to the degree of hydration (and thus density), but range from 120 to 192 nm at 200 eV, and from 193 to 247 nm at 160 eV (i.e., the approximate emission energy for the sulfate spectrum).[23] The investigated films are approximately 100 nm thick; thus, the XES spectra contain information from both, the surface and the bulk of the film (with an exponential weight distribution).

Figure 4 shows S $L_{2,3}$ emission spectra of the three films together with reference spectra of sulfide (CdS), sulfite

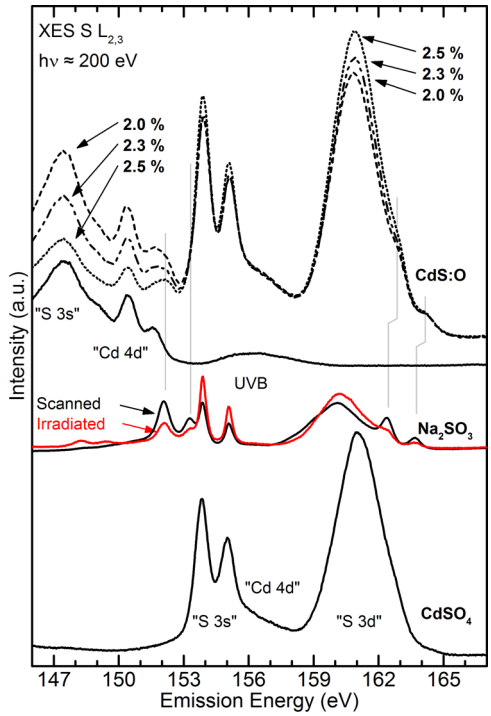

Figure 4. S $L_{2,3}$ X-ray emission spectra of the three CdS:O films with O_2/Ar flow rate ratios of 2.0, 2.3, and 2.5% (top), compared to CdS, $CdSO_4$, and $NaSO_3$ powder references. For the latter, two spectra are shown: with minimal ("scanned") and substantial ("irradiated") beam exposure. Peak labels refer to bands and/or valence orbitals with a strong contribution from the given atomic levels.

(Na_2SO_3), and sulfate ($CdSO_4$) species. S 3s electron decays are seen in two energy regimes.[24−27] For CdS, the broad feature at 147.5 eV is due to the two "S 3s to S $2p_{1/2}$ and $2p_{3/2}$" decay channels in a CdS-like chemical environment (in Figure 4, these transitions are abbreviated as "S 3s" and, correspondingly, "Cd 4d" and "S 3d"). Transitions of S 3s electrons in a $CdSO_4$ chemical environment emit photons at 153.9 and 155.1 eV. Cd 4d-derived valence state decays are also present in both chemical environments, namely at 150.4 and 151.6 eV for CdS and (much less pronounced) at ∼156.5 eV for $CdSO_4$. The peak at 161.0 eV, assigned to states with S 3d contribution,[26,27] is present in the $CdSO_4$ chemical environment, but not found for CdS.

To also gain insights into the possible presence of a sulfite species, we note that $CdSO_3$ is highly unstable and that we therefore used Na_2SO_3 as a reference. The sulfur atom in Na_2SO_3 is predominantly bonded in a molecular fashion, suggesting that the S $L_{2,3}$ emission spectrum of Na_2SO_3 is also a good representative for $CdSO_3$. This assumption is supported by the fact that various different sulfate S $L_{2,3}$ emission spectra look very similar as well.[28] The Na_2SO_3 reference shows a variety of additional peaks, in particular a series of peaks between 151 and 155 eV, as well as two peaks at 162.5 and 163.7 eV, respectively. To identify peaks pertaining to pristine Na_2SO_3, Figure 4 shows two spectra, one recorded with minimal beam exposure by scanning the sample ("scanned"),

DOI: 10.1021/acsami.5b03503
ACS Appl. Mater. Interfaces 2015, 7, 16382−16386

and one after substantial beam exposure, indicating beam-induced changes in the reference sample ("irradiated").

A closer look at the three S $L_{2,3}$ spectra of the here-studied films (top three spectra in Figure 4) reveals a character that is primarily described as a superposition of a sulfide and a sulfate species. Small deviations are found near 152.1 and 153.3 eV, as well as near 162.9 and 164.1 eV. These are ascribed to the most prominent (additional) peaks in the sulfite spectrum, as indicated by the thin vertical lines. Small differential shifts are speculated to be due to a different (molecular) character of the sulfite under study. As indicated by the arrows in Figure 4, an increase of the O_2 flow rate leads to a reduction of the sulfide component and an increase of the sulfate component, while no evidence for a significant change in sulfite contribution can be observed. This is in direct agreement with the findings based on the XPS data of the thin-film surfaces, which exhibit an even larger increase in the sulfate component than the bulk-sensitive XES measurements. This could be due to depth-dependent variations in the composition of the film, but an impact of the XES excitation (i.e., a "sulfate breeding"[29]) can also not be ruled out.

Nevertheless, the existence of three sulfur species (sulfide, sulfate, and intermediate) is found in both XES and XPS, and the comparison with the sodium sulfite reference suggests that the intermediate species might indeed be described as a sulfite (although additional, more complex sulfur compounds could, of course, also be present). By having identified the various components and their relative compositions as a function of O_2 flow rate, it is now possible to optimize the performance of novel CdS:O films, as well as to complement such activities by suitable structure and electronic models based on the species composition of the CdS:O films.

4. SUMMARY AND CONCLUSION

We have studied the chemical and electronic structure of CdS:O thin films produced by incorporating O_2 into the Ar gas flow during sputter deposition. The surface was investigated by XPS, while the bulk of the films were studied by XES. The films were found to be mainly comprised of CdS and $CdSO_4$, with small additions of an intermediate $CdSO_x$ (most likely sulfite) species. With increasing oxygen incorporation, $CdSO_4$ is the preferred species, at the expense of CdS, whereas the content of the intermediate oxide species remains constant. As the oxygen incorporation into the CdS:O films serves several purposes, it is important to understand the composition of such films not just on an atomic level (i.e., composition of Cd, S, and O), but also from the viewpoint of concentration of particular species (i.e., sulfide, sulfate, and intermediate oxide). With such insights, it is now possible to establish suitable models for the CdS:O film properties and their impact on the performance of high-efficiency thin-film solar cells. Furthermore, empirical tailoring toward the optimal balance between the different species can now be quantified and solar cell optimization is thus greatly facilitated.

AUTHOR INFORMATION

Corresponding Authors

*D. A. Duncan. E-mail: Hanksd5@unlv.nevada.edu.
*C. Heske. E-mail: Heske@unlv.nevada.edu.

Present Address

◆Bundeswehr Research Institute for Materials, Fuels and Lubricants (WIWeB), Institutsweg 1, 85435 Erding, Germany

Notes

The authors declare no competing financial interest.

ACKNOWLEDGMENTS

This work was supported by the NSF Accelerated Innovation Research program at Colorado State University, award number 11P-1127362. D. A. Duncan (ne Hanks) gratefully acknowledges financial support through the DAAD RISE Professional program. The ALS is supported by the Department of Energy, Basic Energy Sciences, Contract No. DE-ACo2-05CD11231. R. G. Wilks and M. Bär are grateful to the Helmholtz-Association for financial support (VH-NG-423).

REFERENCES

(1) Green, M. A.; Emery, K.; Hishikawa, Y.; Warta, W.; Dunlop, E. D. Solar Cell Efficiency Tables (Version 45). *Prog. Photovoltaics* **2015**, *23* (1), 1−9.

(2) Sites, J. R. Quantification of Losses in Thin-film Polycrystalline Solar Cells. *Sol. Energy Mater. Sol. Cells* **2003**, *75* (1−2), 243−251.

(3) Wu, X.; Yan, Y.; Dhere, R. G.; Zhang, Y.; Zhou, J.; Perkins, C.; To, B. Nanostructured CdS:O Film: Preparation, Properties, and Application. *Phys. Status Solidi C* **2004**, *1* (4), 1062−1066.

(4) Kephart, J. M.; Geisthardt, R.; Sampath, W. S. Sputtered, oxygenated CdS window layers for higher current in CdS/CdTe thin film solar cells. *Photovoltaic Specialists Conference (PVSC)*, Austin, TX, June 3−8, 2012; IEEE: New York, 2012; pp 854−858.

(5) Kephart, J. M.; Geisthardt, R. M.; Sampath, W. S. Optimization of CdTe Thin-film Solar Cell Efficiency using a Sputtered, Oxygenated CdS Window Layer. *Prog. Photovoltaics* **2015**, n/a.

(6) Islam, M. A.; Sulaiman, Y.; Amin, N. A Comparative Study of BSF Layers for Ultra-Thin CdS:O/CdTe Solar Cells. *Chalcogenide Lett.* **2011**, *8* (2), 65−75.

(7) Paudel, N. R.; Grice, C. R.; Xiao, C. X.; Yan, Y. F. The Effects of High Temperature Processing on the Structural and Optical Properties of Oxygenated CdS Window Layers in CdTe Solar Cells. *J. Appl. Phys.* **2014**, *116* (4), 044506.

(8) Meysing, D. M.; Wolden, C. A.; Griffith, M. M.; Mahabaduge, H.; Pankow, J.; Reese, M. O.; Burst, J. M.; Rance, W. L.; Barnes, T. M. Properties of Reactively Sputtered Oxygenated Cadmium Sulfide (CdS:O) and their Impact on CdTe Solar Cell Performance. *J. Vac. Sci. Technol., A* **2015**, *33* (2), 021203.

(9) Naghavi, N.; Abou-Ras, D.; Allsop, N.; Barreau, N.; Bucheler, S.; Ennaoui, A.; Fischer, C. H.; Guillen, C.; Hariskos, D.; Herrero, J.; Klenk, R.; Kushiya, K.; Lincot, D.; Menner, R.; Nakada, T.; Platzer-Bjorkman, C.; Spiering, S.; Tiwari, A. N.; Torndahl, T. Buffer Layers and Transparent Conducting Oxides for Chalcopyrite Cu(In,Ga)-$(S,Se)_2$ based Thin Film Photovoltaics: Present Status and Current Developments. *Prog. Photovoltaics* **2010**, *18* (6), 411−433.

(10) Kartopu, G.; Clayton, A. J.; Brooks, W. S. M.; Hodgson, S. D.; Barrioz, V.; Maertens, A.; Lamb, D. A.; Irvine, S. J. C. Effect of Window Layer Composition in $Cd_{1-x}Zn_xS$/CdTe Solar Cells. *Prog. Photovoltaics* **2014**, *22* (1), 18−23.

(11) Klenk, R.; Steigert, A.; Rissom, T.; Greiner, D.; Kaufmann, C. A.; Unold, T.; Lux-Steiner, M. C. Junction Formation by Zn(O,S) Sputtering Yields CIGSe-based Cells with Efficiencies Exceeding 18%. *Prog. Photovoltaics* **2014**, *22* (2), 161−165.

(12) Dhere, R. G.; Bonnet-Eymard, M.; Charlet, E.; Peter, E.; Duenow, J. N.; Li, J. V.; Kuciauskas, D.; Gessert, T. A. CdTe Solar Cell with Industrial Al:ZnO on Soda-lime Glass. *Thin Solid Films* **2011**, *519* (21), 7142−7145.

(13) Wu, X.; Dhere, R. G.; Yan, Y.; Romero, M. J.; Zhang, Y.; Zhou, J.; DeHart, C.; Duda, A.; Perkins, C.; To, B. High-efficiency polycrystalline CdTe thin-film solar cells with an oxygenated amorphous CdS (a-CdS:O) window layer. *Photovoltaic Specialists Conference, 2002. Conference Record of the Twenty-Ninth IEEE*, New Orleans, LA, May 19−24, 2002; IEEE: New York, 2002; pp 531−534.

DOI: 10.1021/acsami.5b03503
ACS Appl. Mater. Interfaces 2015, 7, 16382−16386

(14) Soo, Y. L.; Sun, W. H.; Weng, S. C.; Lin, Y. S.; Chang, S. L.; Jang, L. Y.; Wu, X.; Yan, Y. Local Environment Surrounding S and Cd in CdS:O Thin Film Photovoltaic Materials Probed by X-ray Absorption Fine Structures. *Appl. Phys. Lett.* **2006**, *89* (13), 131908.
(15) Seah, M. P. Summary of ISO/TC 201 Standard: VII ISO 15472:2001 - Surface Chemical Analysis - X-ray Photoelectron Spectrometers - Calibration of Energy Scales. *Surf. Interface Anal.* **2001**, *31* (8), 721−723.
(16) Blum, M.; Weinhardt, L.; Fuchs, O.; Baer, M.; Zhang, Y.; Weigand, M.; Krause, S.; Pookpanratana, S.; Hofmann, T.; Yang, W.; Denlinger, J. D.; Umbach, E.; Heske, C. Solid and Liquid Spectroscopic Analysis (SALSA)-a Soft X-ray Spectroscopy Endstation with a Novel flow-through Liquid Cell. *Rev. Sci. Instrum.* **2009**, *80* (12), 123102.
(17) Fuchs, O.; Weinhardt, L.; Blum, M.; Weigand, M.; Umbach, E.; Bar, M.; Heske, C.; Denlinger, J.; Chuang, Y. D.; McKinney, W.; Hussain, Z.; Gullikson, E.; Jones, M.; Batson, P.; Nelles, B.; Follath, R. High-resolution, High-transmission Soft X-ray Spectrometer for the Study of Biological Samples. *Rev. Sci. Instrum.* **2009**, *80* (6), 063103.
(18) Moulder, J.; Stickle, W.; Sobol, P.; Bomben, K. *Handbook of X-ray Photoelectron Spectroscopy*; Perkin-Elmer, Physical Electronics Division: Eden Prairie, MN.
(19) NIST X-ray Photoelectron Spectroscopy Database. http://srdata.nist.gov/xps/.
(20) Briggs, D.; Seah, M. P. *Practical Surface Analysis: Auger and Photoelectron Spectroscopy*, 2nd ed.; John Wiley and Sons: Chichester, U. K., 1990.
(21) Wojdyr, M. Fityk: A General-purpose Peak Fitting Program. *J. Appl. Crystallogr.* **2010**, *43*, 1126−1128.
(22) Scofield, J. H. Hartree-Slater Subshell Photoionization Cross-Sections at 1254 and 1487 eV. *J. Electron Spectrosc. Relat. Phenom.* **1976**, *8* (2), 129−137.
(23) Henke, B. L.; Gullikson, E. M.; Davis, J. C. X-ray Interactions - Photoabsorption, Scattering, Transmission, and Reflection at E-50−30,000 eV, Z-1−92. *At. Data Nucl. Data Tables* **1993**, *54* (2), 181−342.
(24) Weinhardt, L.; Fuchs, O.; Umbach, E.; Heske, C.; Fleszar, A.; Hanke, W.; Denlinger, J. D. Resonant Inelastic Soft X-ray Scattering, X-ray Absorption Spectroscopy, and Density Functional Theory Calculations of the Electronic Bulk Band Structure of CdS. *Phys. Rev. B: Condens. Matter Mater. Phys.* **2007**, *75* (16), 165207−165211.
(25) Weinhardt, L.; Fuchs, O.; Fleszar, A.; Baer, M.; Blum, M.; Weigand, M.; Denlinger, J. D.; Yang, W.; Hanke, W.; Umbach, E.; Heske, C. Resonant Inelastic Soft X-ray Scattering of CdS: A Two-dimensional Electronic Structure Map Approach. *Phys. Rev. B: Condens. Matter Mater. Phys.* **2009**, *79* (16), 165305−165309.
(26) Meisel, A.; Leonhardt, G.; Szargan, R. *Röntgenspektren und Chemische Bindung*; Akademische Verlagsgesellschaft Geest u. Portig: Leipzig, 1977.
(27) Meisel, A.; Steuer, I.; Szargan, R. $L_{2,3}$ X-ray Emission Spectrum of Sulfur in Various Compounds. *Spectrochim. Acta, Part B* **1968**, *B 23* (8), 527−529.
(28) Duncan, D. A. Chemical and Electronic Structure of Surfaces and Interfaces in Cadmium Telluride Based Photovoltaic Devices. Dissertation, University of Nevada, Las Vegas, 2015.
(29) Reichardt, J.; Bar, M.; Grimm, A.; Kotschau, I.; Lauermann, I.; Sokoll, S.; Lux-Steiner, M. C.; Fischer, C. H.; Heske, C.; Weinhardt, L.; Fuchs, O.; Jung, C.; Gudat, W.; Niesen, T. P.; Karg, F. Inducing and Monitoring Photoelectrochemical Reactions at Surfaces and Buried Interfaces in $Cu(In,Ga)(S,Se)_2$ Thin-film Solar Cells. *Appl. Phys. Lett.* **2005**, *86* (17), 172102.

DOI: 10.1021/acsami.5b03503
ACS Appl. Mater. Interfaces 2015, 7, 16382−16386